

Thermal expansion and atomic vibrations of zirconium carbide to 1600 K

A. C. LAWSON*†, D. P. BUTT†‡, J. W. RICHARDSON§ and JU LI¶

†Materials Science and Technology Division,
Los Alamos National Laboratory, Los Alamos, NM 87545, USA

‡Department of Materials Science and Engineering,
Boise State University, Boise, ID 83725, USA

§Intense Pulsed Neutron Source Division,
Argonne National Laboratory, Argonne, IL 60439, USA

¶Department of Materials Science and Engineering,
Ohio State University, Columbus, OH 43210, USA

(Received 13 December 2006; accepted in revised form 12 January 2007)

We have measured the lattice constants and Debye–Waller factors of ZrC from 12 to 1600 K using neutron diffraction. The data have been analyzed with the Grüneisen equation of state using an existing procedure for the Debye–Waller factors and a new procedure for the CTE that takes the temperature dependence of the elastic stiffness into account. The results of these measurements are in good agreement with previous measurements and with recent calculations. We have used the results of our measurements to estimate the melting point of ZrC with the Lindemann rule and obtain an estimate of 4000 K, in good agreement with the measured melting point of 3700 K of this highly refractory material. This last result demonstrates the importance of anharmonic effects in determining the melting point.

1. Introduction

ZrC is one of a large family of highly refractory interstitial compounds with the NaCl-type structure [1]. The Nb(N,C) conventional superconductors and the HfC materials that have the highest known melting point are close relatives. Previous experimental work on ZrC includes thermal expansion measurements by Houska [2], elastic constants and by Chang and Graham [3], phonon spectra by Smith *et al.* [4]. There have been recent calculations of the elastic properties and lattice dynamics by Jochym and Parlinski [5] and of the anharmonic properties by Li *et al.* [6].

We used neutron diffraction to measure the thermal expansion of ZrC with the intention of determining activation energies for carbon vacancy formation using the method of Simmons and Balluffi [7]. In this paper we report thermal expansion and Debye–Waller factor measurements over the temperature range 15–1600 K. The results of these measurements are generally in good agreement with previous measurements and with recent calculations. We analyzed the thermal expansion data

*Corresponding author. Email: aclawson@vla.com

with a new procedure based on the Mie–Grüneisen equation of state that is explained in the appendix to this paper.

2. Experiment

Zirconium carbide powder of particle diameter 20–30 μm was prepared via carbothermic reduction of ZrO_2 in a refractory metal furnace. The powder material was determined by a combination of LECO analysis and combustion to contain less than 100 ppm oxygen. Disks of approximate dimensions 90 mm diameter \times 15 mm thick were prepared by hot pressing the powder at 2100°C, 4000 psi to near theoretical density. Diffraction samples of approximate dimensions 5 \times 5 \times 30 mm³ were cut from the centre of the disks.

Diffraction measurements were made on the general purpose powder diffractometer (GPPD) at the intense pulsed neutron source (IPNS) at Argonne National Laboratory. Low temperature measurements were made using a closed cycle helium refrigerator between 15 and 300 K. High-temperature measurements were made using a special furnace with an alumina tube heated to temperatures between 20 and 1300°C in a helium atmosphere. As the thermal time-constant of this furnace is inconveniently long between 20 and 300°C, data were not collected in that range. Temperatures were determined with Pt–PtRh thermocouples and are believed to be accurate to $\pm 5^\circ\text{C}$.

The design of the furnace permitted measurements with only the $\pm 90^\circ$ detector banks of GPPD, whereas the low-temperature measurements provided data with $\pm 90^\circ$ and the higher resolution $\pm 148^\circ$ detector banks. There was, inevitably, a small discontinuity in the diffractometer calibration at room temperature, and this was removed in the analysis procedure. A second discontinuity in the Debye–Waller factor results was introduced by temporary failure of the furnace at 900°C, and this was accommodated in the standard analysis technique developed for the analysis of the temperature dependence of Debye–Waller factors obtained by pulsed neutron diffraction [8–10]. Diffraction data were analyzed with the general structure and analysis system (GSAS) of Larson and Von Dreele [11].

3. Experimental results

Figure 1 shows the lattice constants of ZrC plotted versus temperature. They are in good agreement with earlier measurements [2] and fair agreement with calculations [6]. The analysis of the ZrC lattice constant data was based on an optimization of equation (A3) from the appendix, modified to accommodate the calibration discontinuity at 300 K. The optimized parameters are the vibrational temperature characteristic of thermal expansion, Θ , the Grüneisen constant γ , and a parameter ξ that is characteristic of the temperature dependence of the

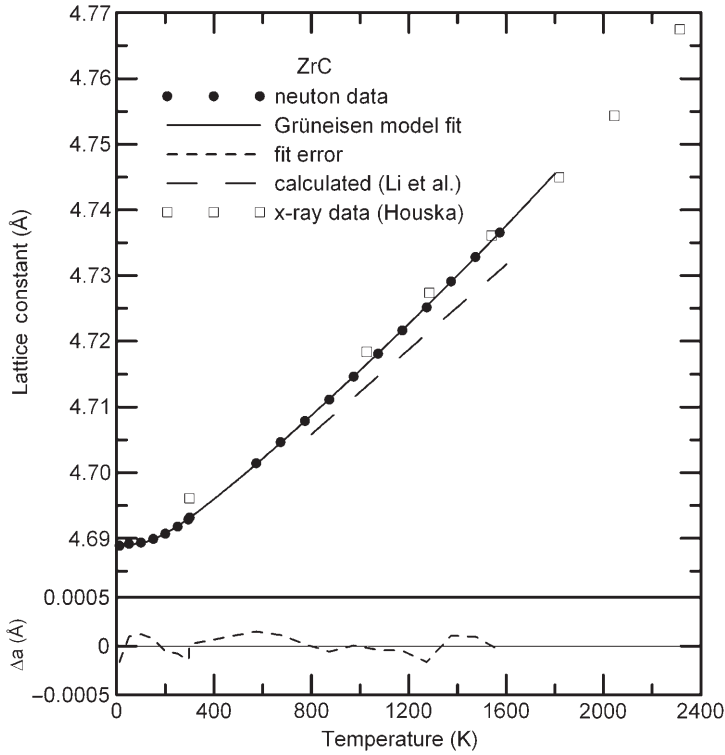


Figure 1. Lattice constants of ZrC, fit to equation (A3) and the error of the fit. Also shown are the experimental points of Houska [2] and calculated points of Li *et al.* [6].

stiffness:

$$\xi = -\frac{1}{\beta B} \left(\frac{\partial B}{\partial T} \right)_P + \left(\frac{\partial \ln \gamma}{\partial \ln V} \right)_T. \quad (1)$$

The result of the optimization for ZrC is $\Theta_{\text{CTE}} = 627(30)$ K and $\gamma = 1.42(2)$ with $\xi = 4.9(5)$. The error in Θ is large, reflecting the insensitivity of the high temperature thermal expansion to Θ . However, the error of the fit is quite small, as shown in figure 1. The fitted parameters are used to calculate the thermal expansion, and the result is shown in figure 2. For comparison, we have also plotted the calculated thermal expansion reported by [6]. In the analysis we have used the value $B = 2.23 \times 10^{12}$ dynes cm^{-2} taken from the literature [2, 4], and a value of V_m derived from the low-temperature lattice constant.

Figure 3 shows the fitted mean-square thermal displacements of the Zr and C atoms plotted versus temperature using a standard definition of $\langle u^2 \rangle$:

$$\langle u^2 \rangle \equiv \frac{(\langle u_x^2 \rangle + \langle u_y^2 \rangle + \langle u_z^2 \rangle)}{3}. \quad (2)$$

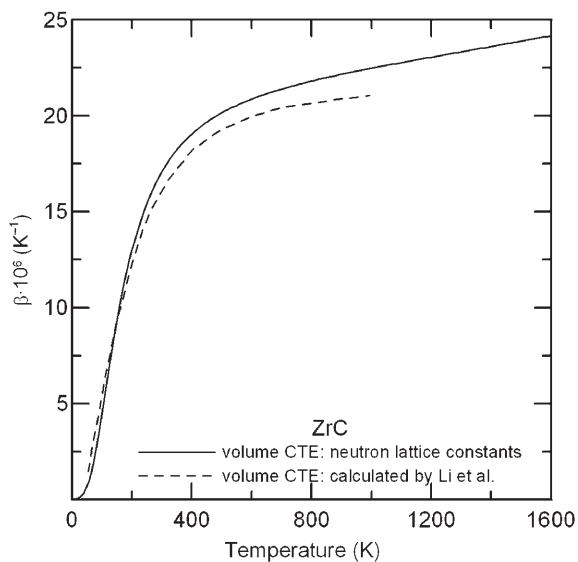


Figure 2. Volume coefficient of thermal expansion (CTE) for ZrC derived from a fit to equation (A3). Also shown is the curve calculated by Li *et al.* [6].

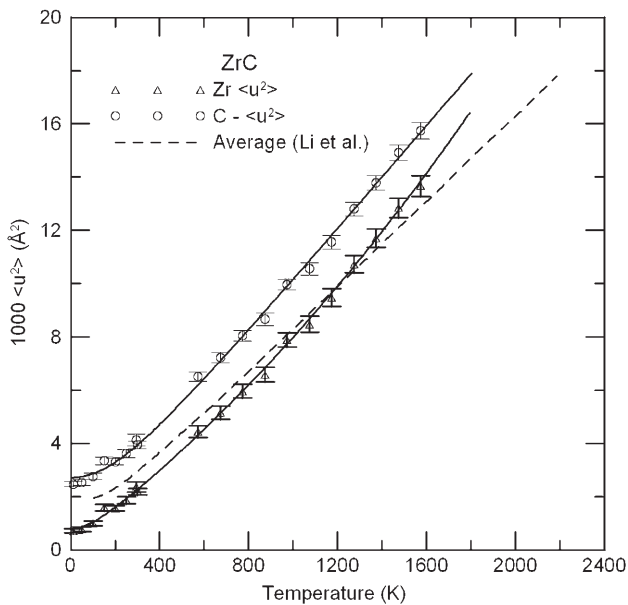


Figure 3. Mean-square atomic thermal displacement ($\langle u^2 \rangle$) for Zr and C in ZrC measured by neutron diffraction. Also shown is the average displacement curve calculated by Li *et al.* [6].

The Debye model is used for both C and Zr; we also tested the Einstein model for the C data, but the Debye model fits are better, as determined by the values of reduced χ^2 . For zirconium, the Debye temperature is somewhat temperature-dependent: $\Theta_{\text{Zr}} = 484(18) - 0.038(9)TK$; for carbon, the the Debye temperature is independent of temperature: $\Theta_{\text{C}} = 1220(11)K$. In an early stage of the refinements, we found that the atom fraction of carbon is independent of temperature; the average value is 1.00(1), and this refinement was subsequently switched off.

The two atomic vibrational frequencies, as measured by the Debye temperatures, are quite different, but the spring constants are about the same, as shown by the ratio:

$$\frac{\Theta_{\text{Zr}}\sqrt{M_{\text{Zr}}}}{\Theta_{\text{C}}\sqrt{M_{\text{C}}}} = 0.91(4). \tag{3}$$

The average Debye temperature is found from the average spring constant:

$$\bar{\Theta} = \frac{\Theta_{\text{Zr}}\sqrt{M_{\text{Zr}}} + \Theta_{\text{C}}\sqrt{M_{\text{C}}}}{\sqrt{M_{\text{Zr}}} + \sqrt{M_{\text{C}}}} = 680(26)K, \tag{4}$$

in reasonable agreement with the value of 627 K found from the thermal expansion.

We can determine atomic Grüneisen constants from the temperature dependences of the Θ : $\Theta = \Theta_0 + cT$. For carbon, we find $\gamma_{\text{C}} = 0$. For zirconium, we find

$$\gamma_{\text{Zr}} = -\frac{c_{\text{Zr}}}{\Theta_{\text{Zr}}\beta} = 3.4(9). \tag{5}$$

For the average Grüneisen constant we have [12]:

$$\bar{\gamma} = \frac{\gamma_{\text{Zr}}C_{\text{Zr}}(T) + \gamma_{\text{C}}C_{\text{C}}(T)}{C_{\text{Zr}}(T) + C_{\text{C}}(T)} \approx \frac{1}{2}\gamma_{\text{Zr}} = 1.7(5). \tag{6}$$

The atomic Grüneisen constants must in principle be somewhat temperature dependent to track the temperature dependences of the heat capacities, but we have neglected this feature in view of the large error of γ_{Zr} . The significant difference between the two atomic Grüneisen constants shows that the anharmonic motion of the Zr atoms is by itself responsible for the thermal expansion of ZrC, and the carbon atoms do not contribute.

4. Comparison with previous work

Data obtained by previous investigators are shown and compared with the present results in table 1. Houska [2] used X-ray diffraction to measure the lattice constants and Debye–Waller factors of ZrC to the very high temperature of 1700°C. We determined the thermal expansion for his data by a linear fit to the lattice constants; his reported Debye–Waller temperature is also shown in table 1. Chang and Graham [3] used ultrasonic methods to obtain the single crystal elastic constants and their temperature dependence over the range 4–300 K. They made

Table 1. Thermoelastic properties of ZrC at 1000 K.

	B (dynes cm ⁻²)	$B^{-1}dB/Dt$ (K ⁻¹)	CTE (K ⁻¹)	γ	ξ	δ	Θ (K)
Calculation [5]	2.3×10^{12}						
Calculation [6]				1.38			747
Elastic (at 300 K) [3]	2.22×10^{12}	-6.25×10^{-5}	21.7×10^{-6}			2.8	714
X-ray lattice constants [2]			19.2×10^{-6}				
Neutron lattice constants ^a			22.4×10^{-6}				
X-ray			22.5×10^{-6}	1.42(2)	4.9(5)		$\Theta_{\text{CTE}} = 627(30)$
Debye-Waller [2]				1.6			614–0.021 T
Neutron							
Debye-Waller ^a				$\bar{\gamma} = 1.7$			$\Theta_{\text{Zr}} = 484 - 0.038 \text{ T}$ $\Theta_{\text{C}} = 1220(11)$ $\bar{\Theta} = 680(26)$ 495(10)
Heat capacity [13]							

^aPresent work.

thermal expansion measurements in the range 4–500 K to provide necessary corrections to their elastic data, but did not report a thermal expansion. We have estimated a CTE by making a linear fit to their graph of thermal expansion. We also determined a value for $B^{-1}(dB/dT)$ from their graphs of the temperature dependence of the elastic constants. Chang and Graham [3] also reported a value for the elastic Debye temperature. Smith *et al.* [4] determined the phonon spectrum of ZrC experimentally using neutron scattering. Their results confirmed the ultrasonic measurements, and no anomalies were found in the spectra. Jocymski and Parlinski [5] calculated the phonon spectrum and obtained good agreement with the measured spectrum of Smith *et al.* [4]. The calculated bulk modulus agrees with that obtained by Chang and Graham [3]. Li *et al.* [6] calculated the phonon frequencies and their volume dependences. From these, they were able to get the Grüneisen constant and the thermal expansion. The present work proceeded in reverse order: we measured the thermal expansion and derived a value for the Grüneisen constant. All of these results are collected in table 1. A calorimetric Debye temperature [13] is included for comparison.

The table shows that our measured thermal expansion is a bit higher than the one calculated by Li *et al.* [6]. If this discrepancy were on the experimental side, a temperature error of the order 10% (measured lower than actual) would be required, and such an error seems to us too large to be credible. Figure 1 includes a comparison of our lattice constants with those obtained by Houska [2] and the thermal expansion results of Li *et al.* [6]. Li *et al.* [6] also calculated the Debye–Waller factors for the zirconium and carbon atoms, and these are in excellent agreement with our experimental results, as shown in figure 3; we have divided their values by three in accordance with our definition of $\langle u^2 \rangle$.

There is considerable disparity among the Debye temperatures reported in table 1. The neutron Debye–Waller temperature for Zr is in good agreement with the Debye temperature from low-temperature heat capacity, but the Debye–Waller temperature for carbon is considerably higher, in accordance with the much lower mass for carbon. As we have already shown, this leads to an average Debye temperature that agrees with the measured Debye temperature for thermal expansion.

The vibrational density of states (DOS) was calculated by Jocymski and Parlinski [5] and by Li *et al.* [6]. In figure 4 we show the vibrational DOS from Li *et al.* [6] together with the DOS from the Debye model used for Debye–Waller and heat capacity data analyses. The DOSs are in general agreement, but the atomic calculations show much finer structure. According to the interpretation given by Li *et al.* [6], nearly all the frequencies below 10 THz are zirconium-like and nearly all above are carbon-like. We may therefore think of the light carbon atoms executing high frequency vibrations inside their zirconium cages.

The γ values in table 1 are in generally good agreement. The value of ξ is nearly twice the value for δ , and equation (1) suggests a large value for $q = (\partial \ln \gamma / \partial \ln V)_T$, the volume variation of the Grüneisen constant. However, comparison of our results for Cu, given in the appendix, to results from the literature, show that values of q obtained from thermal expansion measurements may not be reliable.

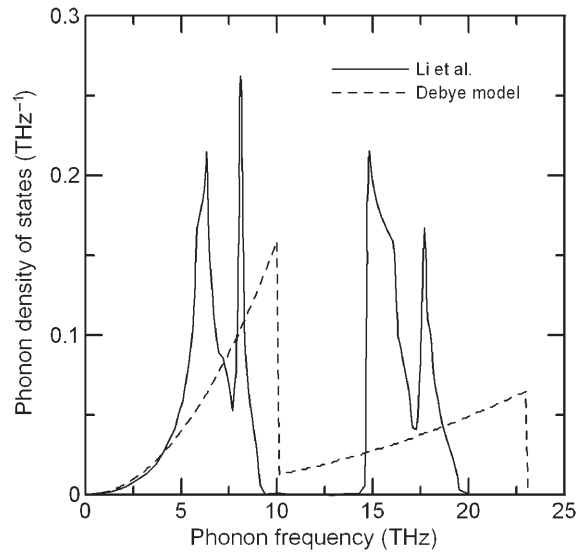


Figure 4. Phonon density of states (DOS) calculated by Li *et al.* [6] compared to the Debye model DOS derived from neutron diffraction data.

5. Lindemann rule and high melting point

With a melting point of 3700 K [14], ZrC is a member of a family of high-melting point materials. HfC has the highest known melting point for a binary, 4160 K [15]. In the absence of a melting theory with a more established physical basis, we can apply the Lindemann melting rule, which states that a material melts when the amplitude of thermal vibration is a small fraction (about 0.08) of the interatomic distance. We have used equations derived previously [16, 17] to estimate the melting point of ZrC. It turns out that it is very important to take the temperature dependence of the Debye temperature into account:

$$T_{\text{melt}} = \frac{f^2 \Omega^{2/3} m k_B \Theta^2}{3 \hbar^2}. \quad (7)$$

In equation (7), f is the ratio of vibrational amplitude to interatomic distance required for melting according to the Lindemann criterion, and Ω is the atomic volume. We take $f=0.08$, as suggested by figure 6 of Lawson [17]. If Θ is temperature dependent, then we have an implicit equation for T_{melt} that can be solved numerically. It is solved explicitly by Lawson *et al.* [16].

On the basis of the data presented in figure 3, we estimate $T_m=4000$ K, which is 8% higher than the observed value. Ignoring the temperature dependence of Θ , we get $T_m=9600$ K, which is more than twice the experimental value. It appears that the melting point in this important family of interstitial carbides is limited by the temperature dependence of the stiffness. (Li *et al.* [6] also estimate a melting point of 4000 K, but their estimate neglects anharmonic effects, and they use a somewhat different formulation of the Lindemann rule.)

6. Discussion and summary

ZrC is a semimetal (its electrical conductivity is about one-third of that of pure Zr), but with strong covalent interactions whose consequences were studied by Li *et al.* [6]. Using a simple 2nd-moment potential (embedded atom) form with isotropic “hopping strengths”, they found it was infeasible to adequately fit the properties of ZrC. Angular interactions are indeed quite strong when one looks at the spatial distribution of forces induced by a small displacement of the Zr or C atom in the lattice, in density functional theory (DFT) calculations. Thus they developed a *pseudo* 2nd-moment potential, where the overall potential form still looks like the 2nd-moment potential, but with angular interactions in the “hopping strength”. Furthermore, to avoid the problem of over-fitting a small DFT data set, they sought a minimal representation of the angular interactions, with the least number of parameters.

Due to the small number of parameters (fitted already to DFT force constants and cohesive energies), we do not expect that significant improvement could be achieved with the present potential form in fitting new properties, without deteriorating some other properties. The philosophy of this potential is to seek a robust 0th-order description, rather than the luxury of achieving high accuracy in a certain property. Having said that, it is probably not too surprising that the finite-temperature vibrational properties of ZrC can be predicted well, since we fitted to the harmonic force constants. This minimal potential form should work with similar quality for TiC, HfC and maybe other semimetals.

In the present work, we found that lattice constants and Debye–Waller factors measured by neutron diffraction are in good agreement with previously reported data and with existing theory. The temperature dependence of the two atomic Debye–Waller factors indicates that the zirconium atoms are much more anharmonic than the light carbon atoms. This anharmonic behaviour, in particular the elastic softening, is responsible for limiting the melting point of ZrC to 3700 K.

Acknowledgments

We are pleased to thank Dr. Hassel Ledbetter for illuminating discussions on the topic of elastic properties and Dr. Jason Lashley for help with one of the references. This research is sponsored by the United States Department of Energy National Nuclear Security Administration and the Office of Science. The work has benefited from the use of the intense pulsed neutron source at Argonne National Laboratory, which is funded by the U.S. Department of Energy, BES-Materials Science, under Contract W-31-109-ENG-38.

Appendix: Thermal expansion analysis and application to copper

We have developed a new procedure for thermal expansion data that will be presented in detail and validated by application to data for copper. Thermal expansion data are often analyzed with the Grüneisen equation

of state [18, 19]:

$$P - P_0 = \frac{\gamma U}{V}$$

where P is the pressure, U is the internal energy and γ is a constant, now known as the Grüneisen constant. U is usually taken from the Debye model with characteristic temperature Θ_D . Taking the temperature derivative at constant volume, it follows that the thermal expansion is proportional to C_v , i.e.

$$\beta = \frac{\gamma C}{BV}$$

When this analysis is made for real materials, it is found that γ is not precisely constant but is rather a weak function of temperature.

Since the temperature variation of the internal energy and heat capacity is usually not known in advance, we assume that these quantities are given by the Debye model and that γ is strictly constant with temperature. We also anticipate that Θ may differ somewhat from the calorimetric Θ_D because the thermal expansion depends more on transverse vibrations [20, 21] than does energy. If measured heat capacity data are available, then the usual thermodynamic Grüneisen constant can be computed by scaling the constant γ by the ratio of the measured heat capacity to the Debye heat capacity. Our assumptions will not work for all materials; in Si, for example, the extra vibrational modes arising from the open structure drive the thermal expansion negative at low temperatures.

As a result of the volume change induced by the thermal expansion, the bulk modulus and Grüneisen constant vary with temperature according to $B = B_0(1 - \beta\delta T)$ and $\gamma = \gamma_0(1 + \beta q T)$, where δ and q are defined by:

$$q \equiv \left(\frac{\partial \ln \gamma}{\partial \ln V} \right)_T,$$

$$\delta \equiv -\frac{1}{\beta B} \left(\frac{\partial B}{\partial T} \right)_p.$$

The quantity δ is the Anderson–Grüneisen constant. The thermal expansion is now given by

$$\left(\frac{\partial V}{\partial T} \right)_p = \frac{\gamma_0(1 + q\beta T)C}{B_0(1 - \delta\beta T)} \approx \frac{\gamma_0 C}{B_0(1 - \xi\beta T)}$$

$$\beta = \frac{\gamma_0(1 + q\beta T)C}{V_0 B_0(1 - \delta\beta T)} \approx \frac{\gamma_0 C}{V_0 B_0(1 - \xi\beta T)}$$

with

$$\xi = \delta + q. \quad (\text{A1})$$

This gives a quadratic equation for β with the solution

$$\beta(T, \Theta, \gamma, \xi) = \frac{1 - \sqrt{1 - 4\xi\gamma C(T, \Theta)T/B_0 V_0}}{2\xi T}. \quad (\text{A2})$$

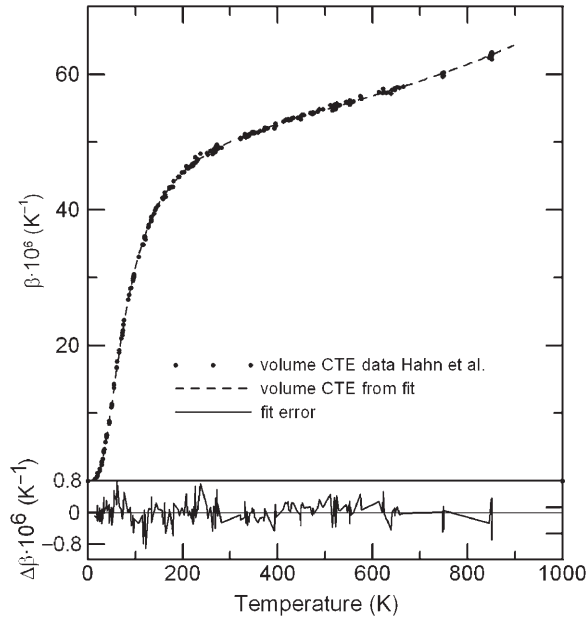


Figure A1. Volume coefficient of thermal expansion (CTE) for copper derived by the application of equation (A3) to the data of Hahn [22].

Given a set of β versus temperature values, a fit to this equation can be optimized for γ , Θ and ξ ; for lattice constants, the optimization can be done with a fit to the integral of equation (A2):

$$V(T, \Theta, \gamma, \xi) = V_0 \left(1 + \int_0^T \frac{1 - \sqrt{1 - 4\xi\gamma C(\tau, \Theta)\tau/B_0V_0}}{2\xi\tau} d\tau \right). \tag{A3}$$

We now test equation (A3) against the high-quality data of Hahn [22] for copper. The fit shown in figure A1 is quite good considering the simplicity of the model. The optimization gives $\Theta_{CTE} = 324.1(5)$ and $\gamma = 1.993(2)$, with $\xi = 4.00(2)$. Values in the literature are $\Theta_D = 343$ K [23] and $\gamma = 1.985$ [24].

In addition to the definition of ξ , there is a relationship [19] between δ and q that involves the pressure derivative $K' = (\partial B/\partial P)$:

$$K' = \delta + 1 - q - \left(\frac{\partial \ln C_V}{\partial \ln V} \right)_T. \tag{A4}$$

The last term in equation (A4) is negligible for $T > \Theta$ and for Cu has the value +0.2 at room temperature.

Depending on how much is known in advance about a given material, several tactics are available for data analysis. Given that ξ and γ are determined from the thermal expansion, one estimates K' from Stacy's version of the Debye model [25] and calculates q and δ by simultaneous solution of equations (A1) and (A4). This is model 1 in table A1. In model 2, an experimental value for δ is taken from the

Table A1. Parameters determined from thermal expansion of copper.

	Model	γ	ξ_{obs}	K'	K'_{γ}	K'_{calc}	δ_{liter}	δ_{calc}	q_{calc}	q_{liter}
Cu	1	1.993(2)	3.99(2)		4.9			3.9	0.0	1.4 ^b
Cu	2		3.99(2)			5.4	4.19(2) ^d		-0.2	3.4 ^c
Cu	3			5.5 ^a			4.19(2) ^d	4.7	-0.2	
ZrC	1	1.42(2)			3.7			3.8	1.1	
ZrC	2		4.9(5)			1.7	2.8 ^e		2.1	

^aDaniels and Smith [26].

^bHoltzapfel *et al.* (experiment) [27, 28].

^cTolpadi, 300 K (calculation) [29].

^dChang and Hultgren [30].

^eChang and Graham [3].

literature, q is estimated from equation (A1) and K' from equation (A4). In model 3, we take an experimental value for K' and use equations (A1) and (A4) for q and δ , respectively. Other routes may be suggested by circumstance. In table A1 we have applied models 1–3 to copper and 1–2 to ZrC. We find that the derived values for δ and q are only in fair agreement with the literature. Perhaps it would be better to have a value for K' measured at $T > \Theta$ and to avoid use of the Debye model altogether.

References

- [1] H.J. Goldschmidt, *Interstitial Alloys* (Plenum Press, New York, 1967), p. 88.
- [2] C.R. Houska, *J. Phys. Chem. Solids* **25** 359 (1964).
- [3] R. Chang and J.J. Graham, *J. Appl. Phys.* **37** 3778 (1966).
- [4] H.G. Smith, N. Wakabayashi and M. Mostoller, in *Superconductivity in d- and f-Band Metals*, edited by D.H. Douglas (Plenum, New York, 1976).
- [5] P.T. Jochym and K. Parlinski, *Eur. Phys. J. B* **15** 265 (2000).
- [6] J. Li, D. Liao, S. Yip, *et al.*, *J. Appl. Phys.* **93** 9072 (2003).
- [7] R.O. Simmons and R.W. Balluffi, *Phys. Rev.* **117** 52 (1960).
- [8] A.C. Lawson, A. Williams, J.A. Goldstone, *et al.*, *J. Less-common Metals* **167** 353 (1991).
- [9] A.C. Lawson, J. A. Goldstone, B. Cort, *et al.*, in *Actinide Processing: Methods and Materials*, edited by B. Mishra and W.A. Averill (TMS, Warrendale PA, 1994).
- [10] A.C. Lawson, J. A. Roberts, B. Martinez, *et al.*, *Phil. Mag. B* **82** 1837 (2002).
- [11] A.C. Larson and R.B. Von Dreele, Los Alamos National Laboratory Report LAUR 86-748 (1986).
- [12] D.C. Wallace, *Statistical Physics of Crystals and Liquids* (World Scientific, New Jersey, 2002), p. 206.
- [13] P. Roedhammer, W. Weber, E. Gmelin, *et al.*, *J. Chem. Phys.* **64** 581 (1976).
- [14] D.P. Butt and T.C. Wallace Sr., *J. Am. Ceram. Soc.* **76** 1409 (1993).
- [15] W.G. Moffatt, *Handbook of Binary Phase Diagrams* (Genium Publishing, Schenectady, NY, 1984).
- [16] A.C. Lawson, B. Martinez, J.A. Roberts, *et al.*, *Phil. Mag. B* **80** 53 (2000).
- [17] A.C. Lawson, *Phil. Mag. B* **81** 255 (2001).

- [18] J. Poirier, *Introduction to the Physics of the Earth's Interior* (Cambridge University Press, Cambridge, 1991).
- [19] O.L. Anderson, *Equations of State of Solids for Geophysics and Ceramic Science* (Oxford University Press, New York, 1996).
- [20] O.L. Anderson, *J. Phys. Chem. Solids* **12** 41 (1959).
- [21] D.F. Gibbons, *Phys. Rev.* **112** 136 (1959).
- [22] T. A. Hahn, *J. Appl. Phys.* **41** 5096 (1970) (Data are available online at: <http://www.itl.nist.gov/div898/handbook/pmd/section6/pmd641.htm>).
- [23] C. Kittel, *Introduction to Solid State Physics*, 7th ed. (Wiley, New York, 1996), p. 126.
- [24] G.K. White, *J. Phys. D* **6** 2070 (1973).
- [25] L. Vočadlo, J.P. Poirier and G.D. Price, *Am. Miner.* **85** 390 (2000).
- [26] W.B. Daniels and C.S. Smith, *Phys. Rev.* **111** 713 (1958).
- [27] W.B. Holzapfel, M. Hartwig and W. Sievers, *J. Phys. Chem. Ref. Data* **30** 515 (2001).
- [28] W.B. Holzapfel, *High Press. Res.* **16** 81 (1998).
- [29] S. Tolpadi, *J. Phys. F* **4** 2138 (1974).
- [30] Y.A. Chang and R. Hultgren, *J. Phys. Chem.* **69** 4162 (1965).